

## Swelling effects in lithium fluoride induced by swift heavy ions

C. Trautmann,<sup>1,\*</sup> M. Toulemonde,<sup>2</sup> J. M. Costantini,<sup>3</sup> J. J. Grob,<sup>4</sup> and K. Schwartz<sup>1</sup>

<sup>1</sup>*Gesellschaft für Schwerionenforschung, Planckstr. 1, D-64291 Darmstadt, Germany*

<sup>2</sup>*CIRIL, CEA/CNRS, BP 5133, 14070 Caen cedex 5, France*

<sup>3</sup>*CEA/SACLAY, BAT 524, DRN/DMT/SEMI, 91191 Gif-sur-Yvette, Cedex, France*

<sup>4</sup>*Laboratoire PHASE, 67037 Strasbourg cedex 2, France*

(Received 18 August 1999)

Using profilometry, large out-of-plane swelling was found when irradiating lithium fluoride with MeV to GeV heavy ions. The effect scales with the range of ions and is linked to the electronic energy loss. Above a critical energy loss of 4.2 keV/nm, ion-induced swelling increases by two to three orders of magnitude. The threshold is much lower than 10 keV/nm required for track etching, suggesting swelling measurements as a suitable technique for testing in particular nonamorphisable material sensitivity versus swift heavy-ion irradiation. A quantitative comparison with data available from x-ray and neutron irradiations indicates that swelling in LiF results from an intermediate defect zone in between the track halo (10–20 nm) consisting mainly of single color centers and the track core (1–2 nm) identified by small-angle x-ray scattering.

In a great number of different materials, radiation induces considerable modifications such as a change of mechanical, electric, optical, and thermal properties. Usually, the effect is based on the ability of energetic radiation to displace atoms directly or via electronic excitation from their equilibrium position and to destroy local order in a crystalline matrix. As a consequence of the damage in the lattice, many irradiated solids react by a change of their volume dimensions. In various materials, whether metals, semiconductors, or insulators, this effect has been studied extensively by using, e.g., x rays, electrons, and neutrons.<sup>1,2</sup>

More recently, considerable swelling was also discovered when irradiating different types of amorphizable oxide crystals [ $\text{Al}_2\text{O}_3$  (Refs. 3–5),  $\text{LiNbO}_3$  (Refs. 6 and 7),  $\text{Gd}_3\text{Ga}_5\text{O}_{12}$  (Ref. 8), and  $\alpha\text{-SiO}_2$  (quartz) (Ref. 9)] with heavy ions of energies in the MeV to GeV range. At such high energies, elastic collisions between the projectile ion and the target atoms can be neglected because the interaction is characterized by almost pure electronic excitation.

In this paper, we report on the appearance of a remarkable out-of-plane swelling in nonamorphizable lithium fluoride. When irradiating single crystals with energetic ions, we had noticed that in many cases the sample surface had bulged outward. At high ion fluences, the effect was sometimes so severe that spontaneous cleaving of the irradiated volume from the unirradiated substrate occurred. In the following, we will present the results of a systematic study using a wide selection of ion species of various energies.

We used 1-mm-thick single crystals of high-purity lithium fluoride cleaved along one of the (100) planes with a polished surface (optical quality). The irradiations were performed with S and Cu ions at the 7 MV Van de Graaff tandem (Bruyères-le-Châtel), with C, O, Mo, and Pb ions at the medium energy line of the GANIL accelerator (Caen), and with Kr, Au, and U ions at the UNILAC of the GSI (Darmstadt). The flux of the ion beam was around  $10^9$  ions  $\text{s}^{-1} \text{cm}^{-2}$  at the tandem Van de Graaff accelerator and between 2 and  $4 \times 10^8$  ions  $\text{s}^{-1} \text{cm}^{-2}$  at the GANIL and GSI accelerators. All samples were irradiated at room temperature and under normal incidence to the sample surface.

About half of the surface area was masked in order to quantify the swelling effects in direct comparison with a virgin area of the same sample. In the given geometry, the ions were stopped in the upper part of the crystal and the free expansion of the irradiated volume is only limited by the constraint of the undamaged substrate. In some cases, thin aluminum foils were placed in front of the crystals to reduce the energy of the ions when impinging on the sample surface. The projected ion range was determined with the computer code TRIM 89 (Ref. 10) and is in good agreement with the thickness of the crystal layer in which color centers are created.<sup>11</sup> Since the observed swelling will result from all defects created along the ion path, the energy loss  $dE/dx$  of a given ion was averaged along the full length of the range. The most relevant parameters of the irradiations are listed in Table I.

The quantitative analysis of the out-of-plane swelling was performed with a profilometer (Dektak 8000) where a high-precision stage moves the sample beneath a diamond-tipped stylus over the border line between the virgin and irradiated areas of the crystal surface. The scans had typically a length of several hundred micrometers. For samples with very large swelling effects, strong bending of the whole crystal occurred and sometimes microcracks at the borderline between the irradiated and virgin area disturbed the step height measurements. The accuracy of the profilometer technique was limited by the roughness (cf. inset of Fig. 1) of the polished surface of approximately 10 nm that allowed us to measure a minimum step height of 10–20 nm. Figure 1 shows the height profiles of samples irradiated with lead and carbon ions (inset) of different fluences. The swelling induced by the carbon ions (11.1 MeV/ $u$ ) led to a step height of only a few tens of nanometers, while a maximum step of more than 700 nm was observed for Pb ions of 4 MeV/ $u$ .

For each sample, a mean step height was extracted from several scans. In the case of light ions (C, O, and S), this averaged step as a function of the ion fluence exhibits a continuous linear increase, although an extremely high fluence of  $2 \times 10^{13}$  ions  $\text{cm}^{-2}$  was applied. For heavier ions, a typical evolution of swelling is presented in Fig. 2. After an

TABLE I. Irradiation parameters [ion species, specific energy (MeV per nucleon), range, maximum applied fluence  $\Phi_{\max}$ , averaged energy loss ( $dE/dx$ )] and experimental data of the initial swelling per ion  $\Delta l/\Delta\Phi$ .

Ion	Energy (MeV/u)	Range ( $\mu\text{m}$ )	$\Phi_{\max}$ (ion/cm <sup>2</sup> )	$dE/dx$ (keV/nm)	$\Delta l/\Delta\Phi$ (cm <sup>3</sup> )
<sup>13</sup> C	11.1	246	$1 \times 10^{13}$	0.6	$3.3 \times 10^{-19}$
<sup>18</sup> O	9.5	166	$1 \times 10^{13}$	1.0	$6.1 \times 10^{-19}$
	5.7	76	$1 \times 10^{13}$	1.4	$3.9 \times 10^{-19}$
<sup>32</sup> S	1.6	12	$2 \times 10^{13}$	4.3	$1.8 \times 10^{-18}$
<sup>36</sup> S	11.2	133	$4 \times 10^{12}$	3.0	$4.3 \times 10^{-18}$
	5.2	46	$4 \times 10^{12}$	4.0	$3.3 \times 10^{-18}$
<sup>63</sup> Cu	1.0	10	$2 \times 10^{13}$	6.1	$3.0 \times 10^{-18}$
<sup>86</sup> Kr	11.4	98	$6 \times 10^{11}$	10.0	$9.0 \times 10^{-17}$
<sup>92</sup> Mo	4.3	35	$1 \times 10^{12}$	11.6	$6.0 \times 10^{-17}$
	1.6	17	$1 \times 10^{13}$	8.8	$7.6 \times 10^{-18}$
<sup>197</sup> Au	2.2	25	$4 \times 10^{11}$	17.3	$4.6 \times 10^{-17}$
	5.4	49	$6 \times 10^{11}$	21.8	$1.1 \times 10^{-16}$
	10.7	89	$4 \times 10^{11}$	23.7	$1.2 \times 10^{-16}$
<sup>208</sup> Pb	4.0	38	$1 \times 10^{12}$	21.9	$1.1 \times 10^{-16}$
	1.8	21	$9 \times 10^{11}$	17.8	$4.5 \times 10^{-17}$
	1.4	18	$1 \times 10^{12}$	16.5	$6.7 \times 10^{-17}$
<sup>209</sup> Bi	3	33	$7 \times 10^{11}$	20.3	$6.1 \times 10^{-17}$
	9	77	$7 \times 10^{11}$	24.6	$1.9 \times 10^{-16}$
<sup>238</sup> U	2.4	30	$2 \times 10^{11}$	19.3	$5.8 \times 10^{-17}$
	3.6	39	$2 \times 10^{11}$	21.8	$8.3 \times 10^{-17}$

initial linear increase, the swelling approaches saturation above fluences of several  $10^{11}$  ions  $\text{cm}^{-2}$ . The saturation effect is attributed to the continuous increase of the irradiated part of the sample surface finally reaching a state when overlapping of the damage zones of single tracks becomes significant. Such a situation can be described by a Poisson law<sup>11</sup> from which the radius of the damage zone contributing to swelling can be deduced. A fit to our Pb data (solid line in Fig. 2) gives a swelling radius of about 7 nm. For most other irradiations, the number of high-fluence data is too limited for a quantitative analysis.

Another interesting observation concerns the influence of the irradiation parameters. For ions with approximately the

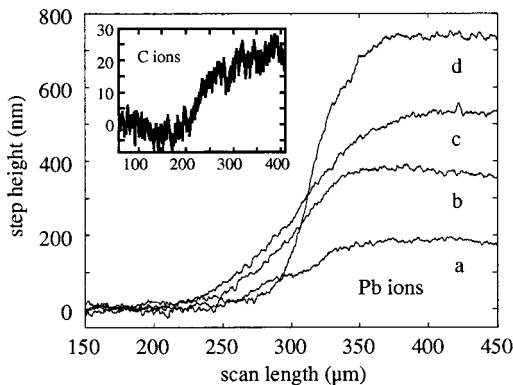


FIG. 1. Profilometer scans from virgin (left) to irradiated (right) area of crystals exposed to Pb (4 MeV/u) of (a)  $1.2 \times 10^{11} \text{ cm}^{-2}$ , (b)  $3 \times 10^{11} \text{ cm}^{-2}$ , (c)  $6 \times 10^{11} \text{ cm}^{-2}$ , and (d)  $1.2 \times 10^{12} \text{ cm}^{-2}$  and to C ions (11.1 MeV/u) of  $6 \times 10^{12} \text{ cm}^{-2}$  (inset).

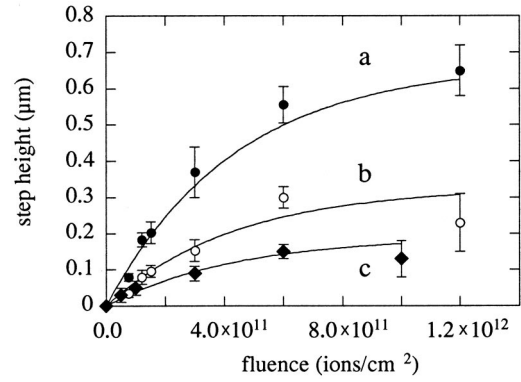


FIG. 2. Step height as a function of the fluence for irradiations with (a) Pb (4 MeV/u), (b) Pb (1.4 MeV/u), and (c) Mo (4.3 MeV/u) ions.

same range, the swelling scales with the mean energy loss (cf. curves *a* and *c* in Fig. 2) and for ions of approximately the same mean energy loss [cf. Table I, <sup>32</sup>S (1.6 MeV/u) and <sup>36</sup>S (5.2 MeV/u)], the step height per ion is higher for larger ranges. These observations are in good agreement with earlier findings.<sup>3,7-9</sup>

In order to compare the swelling of different ion species, the relative contribution of a single ion plotted as a function of the mean energy loss is presented in Fig. 3 (the uncertainty of the energy loss is assumed to be 15% and for clarity reasons not shown for all data). For this, the initial swelling rate  $\Delta l/\Delta\Phi$  was deduced from the slope of the step height in the linear fluence regime (cf. Table I). In a first approximation, this value was normalized by the projected ion range. We chose a semilogarithmic scale to underline the extremely small swelling effect of carbon ions and the increase by two to three orders of magnitude for heavier ions of energy losses larger than 4 keV/nm. In a linear presentation, a straight line fits to the experimental data intercepting the abscissa at an energy loss of  $(dE/dx)_c = 3.2 \pm 1.1 \text{ keV/nm}$ . This value can be regarded as a threshold that has to be surpassed before the dimensional change can occur. It also tells us that for a region of typically 1–3  $\mu\text{m}$  close to the stopping end of the ion path (and for the <sup>36</sup>S ions of 11.2 MeV/u also a larger region close to the crystal surface), the critical energy loss is not reached and therefore does not contribute to swelling. This effect was taken into account by subtracting for each ion the

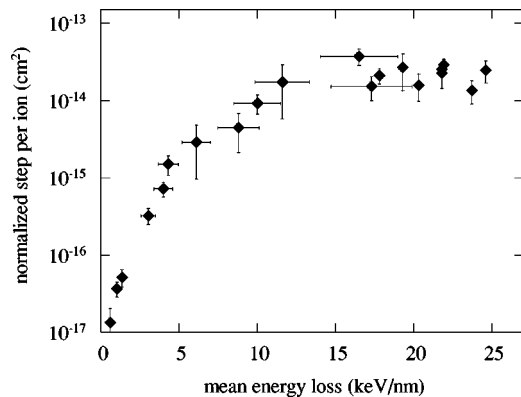


FIG. 3. The initial swelling ( $\Delta l/\Delta\Phi$ ) normalized by the ion range vs the mean energy loss.

subthreshold part of the trajectory from the projected range. As in earlier studies,<sup>8,9</sup> the value for the normalized swelling and for the mean energy loss was adjusted in several steps by an iterative procedure. It finally leads to a slightly higher threshold value of  $(dE/dx)_c = 4.2 \pm 1.4$  keV/nm. Local variations of track parameters such as discontinuity, inhomogeneity of the damage, or change of the track radius along the ion path do not influence this result since the volume swelling is an effect integrated along the full length of the damaged ion path.

We tried to complement the present profilometer measurement by using other physical characterization techniques, e.g., Rutherford backscattering under channeling condition (RBS/C). Unfortunately, a reliable analysis turned out to be problematic because LiF crystals are very radiation sensitive and therefore easily damaged under the bombardment with  $\alpha$  particles.<sup>12</sup> The same argument applies for high-resolution electron microscopy, making direct imaging of tracks in LiF very difficult. Finally, the surface of ion-irradiated LiF was studied by atomic force microscopy (AFM),<sup>13</sup> imaging the impact zones of single ions as hillocks with a few nanometers in height and several tens of nanometers in diameter. The volume of such hillocks is by one to two orders of magnitude smaller than the volume change per ion observed when scanning with the profilometer tip from the virgin to the irradiated crystal area (cf.  $\Delta I/\Delta\Phi$  in Table I).

In this section, we shall discuss possible explanations for ion induced swelling. In the case of oxide materials [e.g.,  $\text{Gd}_3\text{Ga}_5\text{O}_{12}$  (Refs. 8, 14, and 15) and  $\alpha$ - $\text{SiO}_2$  (Refs. 9 and 16)], the situation is rather straight forward because swelling can be interpreted as a change of density due to a transition from the crystalline to the amorphous phase.<sup>14–17</sup> In addition, the energy loss threshold of swelling is in good agreement with the threshold for amorphisation as determined by RBS/C (Refs. 8, 9, and 14–16) in combination with high-resolution electron microscopy.<sup>14–16</sup> In LiF, the situation is different because amorphization is not expected for crystals with such a strong ionic binding character. It is more likely that swelling originates from the formation of specific defects. In a series of recent experiments,<sup>11,18,19</sup> it was shown that ion tracks in LiF have a rather complex damage structure, namely, a track core with defect clusters surrounded by a much larger halo with mainly single color centers. Similar as under conventional radiation, all species of ions create single defects around the ion trajectory in a region of up to several tens of nanometers. The situation is different for the track core which is exclusively created by heavy projectiles. The existence of this core has been evidenced by a highly anisotropic small-angle x-ray scattering (SAXS) pattern and is ascribed to a change of the electron density within a cylinder radius of 1–2 nm.<sup>11,18</sup> Most likely, defect clusters in this narrow track zone are also responsible for the fact that above a critical energy loss of 10 keV/nm, tracks of heavy ions can be attacked by a suitable etchant.<sup>20–23</sup> Although the nature of this specific damage induced by heavy ions has not been uncovered so far, it is assumed that defect aggregates such as small Li colloids and fluorine and vacancy clusters are responsible for the observed effects.

For a more quantitative analysis of the here described swelling, we compared our results with structural expansion

data due to conventional radiation. In a dose regime that is dominated by the creation of single Frenkel defects, detailed experimental data are available from x-ray diffraction, dilatometry, and high-precision density measurements.<sup>24</sup> The contribution of single Frenkel defects in our samples was deduced by measuring the  $F$ -center concentration using optical absorption spectroscopy. If we assume that the relative change  $\Delta l/l$  of the linear dimension of the crystal corresponds to the relative volume change, the  $F$  centers due to the irradiation with carbon and oxygen ions lead to a step height in good agreement with our profilometer measurement. The situation is quite different for heavier ions with a stopping power larger than 4 keV/nm where the volume expansion due to the creation of color centers is by one or two orders of magnitude smaller than the swelling observed. The contribution of small aggregate centers (e.g.,  $F_2$  or  $F_3$  centers) is also not significant because their concentration is always much smaller. We conclude that single defects (or small aggregates) in the track halo of heavier-ion species do not give a significant contribution to the swelling observed here.

Another estimation can be made, considering data available from high-dose irradiations with thermal neutrons up to a fluence of  $10^{20}$  cm<sup>-2</sup>.<sup>25,26</sup> The radiation damage mainly originates from  $\alpha$  and tritium particles from fission processes [ $^6\text{Li}(n, \alpha)^3\text{H}$ ], resulting in a homogeneous dose distribution in the entire crystal volume. It was demonstrated that up to a fluence of  $2 \times 10^{17}$  neutrons cm<sup>-2</sup> (corresponding to a dose of about 10 MGy and a volume increase of less than 0.6%), swelling increases linearly with the number of Frenkel pairs, whereas at higher doses nonlinear effects appear. They are ascribed to the formation of more complex defects such as molecular fluorine inclusions and lithium colloids. For a comparison of our results with the neutron data, we consider the Pb irradiation in the linear fluence regime (cf. Fig. 2) at  $3 \times 10^{11}$  ions cm<sup>-2</sup>, corresponding to a total dose of about 4 MGy. In this situation, the ion induced swelling  $\Delta l/l$  is around 1.2%. If we assume that this  $\Delta l/l$  corresponds to the total volume increase relaxed towards the sample surface, such a swelling is reached by neutron irradiation only for a dose above 30 MGy. Concluding this estimation, it should be emphasized that a direct comparison of the ion and neutron irradiation is certainly problematic because it does not consider that each ion deposits the energy with a radial distribution of approximately  $1/r^2$  (where  $r$  is the radial distance from the ion trajectory).

In order to take into account the radial distribution of the deposited energy, some known parameters of the track size can be used for a quantitative estimate of the swelling of a single track. According to SAXS experiments, the track core of Pb ions has a radius of about 1.5 nm.<sup>11</sup> Based on model calculations,<sup>11,27,28</sup> it can be assumed that for each individual track only 30% of the total energy is deposited in this small cylindrical core. For Pb ions of 4 MeV/ $u$ , this corresponds to a dose of about 70 MGy. At such a high dose, neutron-induced volume swelling has reached a saturation value of approximately 20%, while  $\Delta l/l$  (as estimated from the data in Table I) gives almost 60% for the track core of Pb ions. Such a large value of swelling does not seem to be of realistic significance strongly suggesting that the zone contributing to swelling must be larger than the SAXS radius. A first

evidence for such an intermediate swelling radius is obtained from the fit of the swelling data of Pb ions in Fig. 2, where a radius of about 7 nm can well describe the saturation behavior. In addition, assuming intermediate swelling radius, the volume increase of each track corresponds to 2.6% (for a dose of 6 MGy deposited in the track), which seems to be more reasonable.

Concluding our results, it has to be pointed out that above a linear energy transfer of 4.2 keV/nm, the irradiation of LiF with heavy ions leads to an unexpected large volume expansion. The resulting out-of-plane swelling scales with the range and with the energy loss of the projectiles. The effect is about one to two orders of magnitude larger than expected from single Frenkel pairs. Consequently, it is reasonable to assume that single defects do not contribute significantly but mainly defect clusters such as small Li colloids and vacancy and molecular fluorine clusters are responsible for ion-induced swelling.

A quantitative comparison with data from conventional radiations and track parameters known from SAXS experiments indicates that the zone responsible for swelling corresponds to a cylinder with an intermediate radius, i.e., smaller than the zone in which mainly  $F$  centers are created, but significantly larger than the SAXS radius.

The second important finding is that specific radiation effects due to collective electronic excitation processes in heavy-ion tracks can be evidenced via swelling experiments. In LiF this occurs at a much lower energy loss than revealing of ion tracks by chemical etching ( $dE/dx = 10$  keV/nm). It should be emphasized that profilometry as an extremely sensitive and destruction-free method seems to be in particular suitable for nonamorphizable materials which are difficult to study by other means.

We would like to thank F. Eisele for his contribution to the profilometer measurements.

---

\*Corresponding author. FAX: +49-6159-712179. Email address: C.Trautmann@gsi.de

<sup>1</sup>D. S. Bilington and J. H. Crawford, in *Radiation Damage in Solids* (Princeton University Press, Princeton, 1961).

<sup>2</sup>K. Tanimura, T. Tanaka, and N. Itoh, *Phys. Rev. Lett.* **51**, 423 (1983).

<sup>3</sup>R. Brenier, B. Canut, S. M. M. Ramos, and P. Thévenard, *Nucl. Instrum. Methods Phys. Res. B* **90**, 339 (1994).

<sup>4</sup>S. M. M. Ramos, N. Bonardi, B. Canut, and S. Della-Negra, *Phys. Rev. B* **57**, 189 (1998).

<sup>5</sup>S. M. M. Ramos, N. Bonardi, B. Canut, S. Bouffard, and S. Della-Negra, *Nucl. Instrum. Methods Phys. Res. B* **143**, 319 (1998).

<sup>6</sup>B. Canut, R. Brenier, A. Meftah, P. Moretti, S. Ould Salem, S. M. M. Ramos, P. Thévenard, and M. Toulemonde, *Nucl. Instrum. Methods Phys. Res. B* **91**, 312 (1994).

<sup>7</sup>B. Canut, S. M. M. Ramos, R. Brenier, P. Thévenard, J. L. Loubet, and M. Toulemonde, *Nucl. Instrum. Methods Phys. Res. B* **107**, 194 (1996).

<sup>8</sup>M. Toulemonde, A. Meftah, J. M. Costantini, K. Schwartz, and C. Trautmann, *Nucl. Instrum. Methods Phys. Res. B* **146**, 426 (1998).

<sup>9</sup>C. Trautmann, J. M. Costantini, A. Meftah, K. Schwartz, J. P. Stoquert, and M. Toulemonde, in *Atomistic Mechanisms in Beam Synthesis and Irradiation of Materials*, edited by J. C. Barbour, S. Roorda, D. Ila, and M. Tsujioka, MRS Symposia Proceedings No. 504 (Materials Research Society, Pittsburgh, 1999), p. 123.

<sup>10</sup>J. F. Ziegler, P. Biersack, and U. Littmark, in *The Stopping and Ranges of Ions in Matter*, edited by J. F. Ziegler (Pergamon, New York, 1985).

<sup>11</sup>K. Schwartz, Ch. Trautmann, T. Steckenreiter, O. Geiss, and M. Krämer, *Phys. Rev. B* **58**, 11 232 (1998).

<sup>12</sup>M. J. Hollis, C. S. Newton, and P. B. Price, *Phys. Lett.* **44A**, 243 (1973).

<sup>13</sup>A. Müller, R. Neumann, K. Schwartz, T. Steckenreiter, and C. Trautmann, *Appl. Phys. A: Mater. Sci. Process.* **66**, S1150 (1998); A. Müller, R. Neumann, K. Schwartz, and C. Trautmann, *Nucl. Instrum. Methods Phys. Res. B* **146**, 393 (1998).

<sup>14</sup>J. M. Costantini, F. Ravel, F. Brisard, M. Caput, and C. Cluzeau, *Nucl. Instrum. Methods Phys. Res. B* **80/81**, 1249 (1993).

<sup>15</sup>J. M. Costantini, F. Brisard, L. Autissier, M. Caput, and F. Ravel, *J. Phys. D* **26**, A57 (1993).

<sup>16</sup>A. Meftah, F. Brisard, J. M. Costantini, E. Dooryhee, M. Hage-Ali, M. Hervieu, J. P. Stoquert, F. Studer, and M. Toulemonde, *Phys. Rev. B* **49**, 12 457 (1994).

<sup>17</sup>L. Douillard, F. Jollet, J. P. Duraud, R. A. B. Devine, and E. Dooryhee, *Radiat. Eff. Defects Solids* **124**, 351 (1992).

<sup>18</sup>C. Trautmann, K. Schwartz, J. M. Costantini, T. Steckenreiter, and M. Toulemonde, *Nucl. Instrum. Methods Phys. Res. B* **146**, 367 (1998).

<sup>19</sup>A. Perez, E. Balanzat, and J. Dural, *Phys. Rev. B* **41**, 3943 (1990).

<sup>20</sup>D. A. Young, *Nature (London)* **182**, 375 (1958).

<sup>21</sup>K. Schwartz, *Nucl. Instrum. Methods Phys. Res. B* **107**, 128 (1996).

<sup>22</sup>C. Trautmann, K. Schwartz, and O. Geiss, *J. Appl. Phys.* **83**, 3560 (1998).

<sup>23</sup>K. Schwartz, G. Wirth, and C. Trautmann, *Phys. Rev. B* **56**, 10 711 (1997).

<sup>24</sup>R. Balzer, H. Peisl, and W. Waidelich, *Phys. Status Solidi* **15**, 495 (1966).

<sup>25</sup>J. Spaepen, *Phys. Rev. Lett.* **1**, 281 (1958).

<sup>26</sup>H. Peisl, W. Kapfhammer, and W. Waidelich, *Solid State Commun.* **2**, 167 (1964).

<sup>27</sup>M. Krämer and G. Kraft, *Radiat. Environ. Biophys.* **33**, 91 (1994).

<sup>28</sup>M. P. R. Waligorski, R. N. Hamm, and R. Katz, *Nucl. Tracks Radiat. Meas.* **11**, 309 (1986).